JIRRS
Journal International Review of Research Studies

Received: 13/06/2026 - **Accepted:** 13/11/2026
Vol: 1.11
DOI: 10.66104/gtgx0451
Pages: 1-32

Pneumatic Classification of Dry-Ground Minerals: Fundamentals, Equipment Technologies and Separation Performance

Antonio Clareti Pereira, PhD
PhD in Chemical Engineering
University of São Paulo (USP)
Belo Horizonte, Minas Gerais, Brazil
E-mail: claretipereira@gmail.com
ORCID: https://orcid.org/0000-0001-8115-4279

Abstract

Pneumatic classification governs the product-size distribution and material selectivity of dry mineral processing, yet published performance comparisons often combine dissimilar feeds, separation metrics, and operating boundaries. This critical review examines particle transport, gravitational and centrifugal mechanisms, dynamic rotor technologies, partition-curve interpretation, and measurement uncertainty, using a structured bibliography of 124 publications mainly from 2010 to 2026. Rather than treating cut size as an equipment constant, the synthesis frames it as a joint outcome of airflow, rotor geometry and speed, solids loading, particle density and morphology, agglomeration, and sampling protocols. Reported fish-hook behavior and bypass demonstrate that an apparently favorable median cut does not necessarily imply sharp separation. Studies of pilot and industrial classifiers further indicate that pressure loss, process stability, and representative sampling must be assessed together with product fineness. The distinctive contribution is a measurement-centered validation framework integrating classwise material closure, sampling bias, component-resolved partitioning, bypass and fish-hook diagnostics, and matched-duty technology comparison. The bibliography is a curated source dataset rather than a verified systematic-review corpus; quantitative meta-analysis is therefore not claimed.

Keywords: pneumatic classification; dry mineral processing; dynamic air classifier; partition curve; fish-hook effect; classification sharpness

Highlights

- Cut size must be interpreted jointly with bypass, sharpness, and mass-balance closure.
- Classifier rankings change with feed density, fines agglomeration, and loading.
- Measured partition curves are vulnerable to size-dependent sampling and entrainment bias.
- Technology selection requires separation performance and pressure-loss evidence at matched conditions.

JIRRS
Journal International Review of Research Studies
Received: 13/06/2026 - **Accepted:** 13/11/2026
Vol: 1.11
DOI: 10.66104/gtgx0451
Pages: 1-32

Graphical Abstract

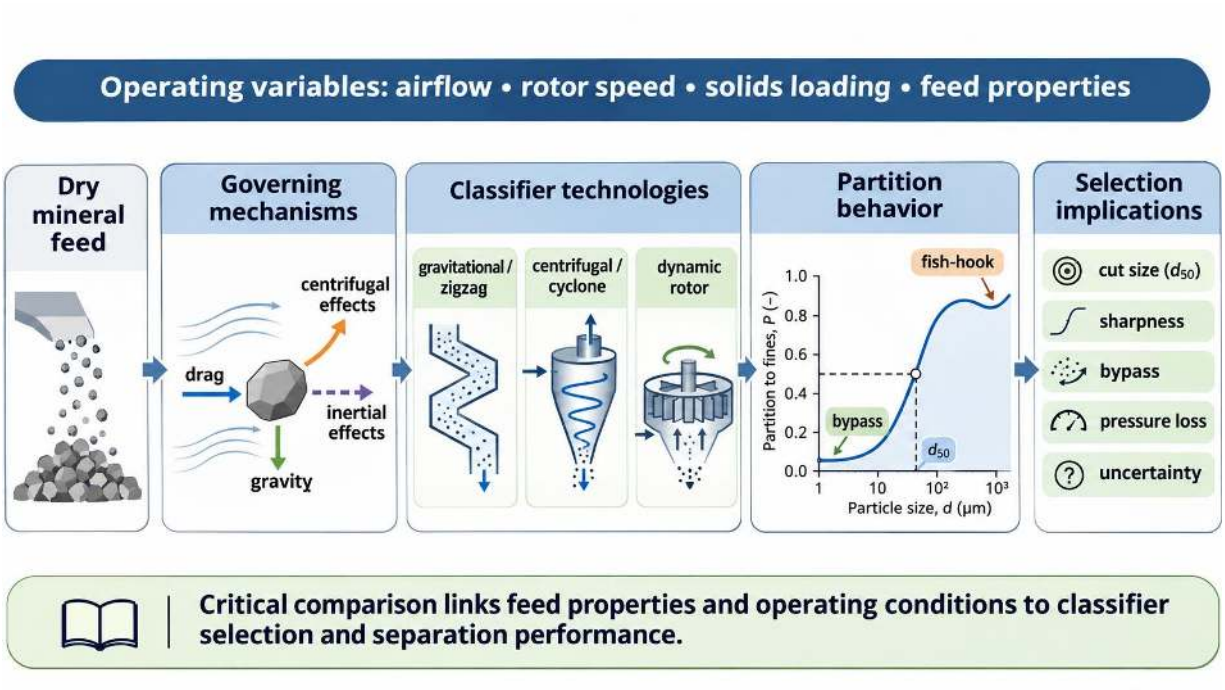

Graphical abstract. Conceptual framework linking mechanisms, performance metrics, and technology selection.

Note. Original conceptual illustration developed for this review with image-generation assistance; no experimental data are represented. All curves, labels, and equipment schematics are illustrative and do not establish measured performance. Disclosure remains subject to the journal's image-generation policy.

1. Introduction and Industrial Motivation

Dry comminution requires deliberate control of particle-size distribution (PSD), particularly where excess fines degrade downstream handling or where wet separation adds unacceptable water use. Pneumatic classifiers exploit aerodynamic particle response to split streams without a slurry phase, but their performance cannot be reduced to the nominal classifier cut size alone. Feed composition and particle morphology shift the effective operating envelope, and cross-study comparisons require explicit definitions of the system boundary (Altun, 2022; Altun & Benzer, 2014; Altun et al., 2016; Ansari et al., 2025; Cepuritis et al., 2015; Eswaraiah et al., 2019; Huang et al., 2026).

The industrial question is not merely whether an air classifier can remove fines, but whether it can deliver a reproducible product quality at practical throughput, energy demand,

JIRRS
Journal International Review of Research Studies
Received: 13/06/2026 - **Accepted:** 13/11/2026
Vol: 1.11
DOI: 10.66104/gtgx0451
Pages: 1-32

and material losses. Dynamic rotor systems offer adjustable separation conditions, whereas gravitational and cyclone-based systems can be more robust or better suited to coarser separation tasks. Published model, experimental, and industrial reports should therefore be interpreted as complementary, not interchangeable, evidence (Jia et al., 2021; Kundu et al., 2021; Peng et al., 2022; Petit & Irassar, 2021; Pukkella et al., 2023; Tipici et al., 2024; Vokurka et al., 2025).

Recent reviews by Pukkella et al. (2023) and Huang et al. (2026) comprehensively address classifier mechanisms, equipment evolution, flow-field optimization, CFD/DEM, energy, and scale-up. The present critical review does not claim priority for that broad synthesis. Instead, it offers a measurement- and evidence-centered framework: a defined coarse-product partition convention; reconciled total and classwise dry-solids balances; diagnostics for fine-end bypass and fish-hook behavior; component-resolved aerodynamic response; representative, uncertainty-aware sampling; and technology benchmarking under matched feed, duty, and energy boundaries. Ansari et al. (2025) illustrate industrial troubleshooting and why feed distribution, dust management, bag filters, and control conditions must be evaluated as a single process system.

Table 1 summarizes equipment classes as analytical categories rather than claiming universal numerical performance limits. Figures 1 and 3 establish the force-balance and partition-curve conventions used throughout, and Table 3 defines the minimum performance indicators. The scope is limited to classifier physics and technology performance; mill circuit design is considered only when needed to define the classifier boundary.

Table 1. Mechanistic comparison of dry classifier families.

Classifier family	Principal driving mechanism	Strength / suitable question	Principal limitation
Gravity / zigzag	Gravity, drag, repeated cross-flow	Coarse segregation; multistage sorting	Turbulence and orientation effects
Cyclone / centrifugal	Tangential inertia and gas drag	Compact, continuous treatment	Short-circuiting and pressure loss
Dynamic rotor/cage	Radial drag versus rotor-induced inertia	Adjustable fine cut and PSD control	Rotor power; loading sensitivity
Hybrid/multistage	Sequential forces and re-entrainment	Targeted product splitting	More complex sampling and controls

JIRRS
Journal International Review of Research Studies
Received: 13/06/2026 - **Accepted:** 13/11/2026
Vol: 1.11
DOI: 10.66104/gtgx0451
Pages: 1-32

Note. Qualitative synthesis from the supplied bibliography. No universal cut-size limits are asserted without matched feed conditions.

2. Review Methodology, Questions, and Evidence Grading

This critical narrative review evaluates pneumatic classification mechanisms, equipment design, separation performance, and uncertainty using a compiled bibliography of 124 records, primarily dated 2010–2026. The search terms and thematic categories were organized around eleven research questions; however, the underlying retrieval records and complete full-text screening log were not available for independent replication. Consequently, we treat the bibliographic collection as a curated source set, not a systematically retrieved or exhaustively screened population of publications.

The review was updated for the present revision on 9 November 2026; this is the manuscript update date, not a claim of a new reproducible database-search run. The source collection was supplied as a preassembled bibliography; the available records do not allow us to establish the original search dates, databases, or search-engine execution logs. Thus, no database-specific retrieval counts, PRISMA flowchart, or independently completed full-text/DOI audit are claimed. Representative reproducible search expressions for subsequent verification are: ("air classifier" OR "pneumatic classification") AND (mineral* OR ore*); ("partition curve" OR "Tromp curve") AND (bypass OR "fish hook"); ("dynamic classifier" OR "rotor classifier") AND (CFD OR DEM OR validation); and ("dry classification" AND (sampling OR uncertainty OR "mass balance")). These are indicative strategies, not retrospectively asserted executed searches.

The evidence was organized by proximity to mineral-classification practice: industrial measurements, pilot and laboratory tests, independently validated simulations, unvalidated simulations, and analogous studies on non-mineral powders. This ordering does not assume that every industrial study is better controlled than every laboratory experiment; traceable sampling, mass closure, and independent validation govern the weight of individual results. Where operating boundaries or test feeds differ, the comparison remains qualitative.

The evidence hierarchy separates industrial field measurement from pilot-scale trials, laboratory experiments, calibrated modeling, unvalidated simulation, and narrative synthesis.

JIRRS
Journal International Review of Research Studies
Received: 13/06/2026 - **Accepted:** 13/11/2026
Vol: 1.11
DOI: 10.66104/gtgx0451
Pages: 1-32

Performance claims are weighted by observed material closure, replicate sampling, stated classifier geometry, reported particle-density distribution, and the completeness of partition data. Benchmarking and review sources clarify terminology but cannot substitute for independent measurement (Fu et al., 2024; Huang et al., 2026; Kaas et al., 2022; Otwinowski et al., 2022; Pukkella et al., 2023; Roloff et al., 2019; Yoshida et al., 2021).

Three questions structure the comparison: (i) how do particle density and shape change the effective cut; (ii) when do observed bypass and fish-hook features indicate classifier transport rather than biased measurement; and (iii) which operating conditions yield a narrow product-size distribution at a stated solids throughput? Apparent agreement between studies is not treated as quantitative equivalence unless feed characteristics, partition conventions, and system boundaries can be compared.

The eleven guiding questions are: (1) Which aerodynamic mechanisms govern segregation? (2) How do classifier geometries alter transport? (3) How are apparent and corrected cuts defined? (4) How should bypass be diagnosed? (5) When is fish-hook curvature credible? (6) How do airflow and rotor speed interact? (7) How does solids loading modify partitioning? (8) How do density, shape, moisture, and agglomeration change aerodynamic response? (9) What sampling and closure checks are necessary? (10) How should simulations and industrial measurements be graded? (11) How can technologies be benchmarked at matched feed, product duty and energy boundaries? Evidence classes are A: industrial mineral classification with field measurement; B: pilot/laboratory mineral classification; C: independently validated simulations; D: non-mineral analog experiments; and E: unvalidated models or concepts. Classification is a transparency aid, not a numerical quality score.

3. Drag, Terminal Velocity, and Cut-Size Fundamentals

A particle responds to the local relative velocity between gas and solids, not to the nominal superficial airflow alone. In a dilute flow, resistance depends on drag coefficient, projected area, gas density, and the square of slip velocity. The effective terminal or radial transport condition is modified by particle Reynolds number, non-sphericity, turbulence, wall proximity, and interparticle forces. As loading rises, collective motion and local gas-velocity

JIRRS
Journal International Review of Research Studies
Received: 13/06/2026 - **Accepted:** 13/11/2026
Vol: 1.11
DOI: 10.66104/gtgx0451
Pages: 1-32

redistribution undermine independent-particle approximations (Bagherzadeh et al., 2024; Barimani et al., 2018; Caliskan et al., 2019; Fu et al., 2016; Gao et al., 2013; Huang et al., 2024a; Huang et al., 2012; Johansson & Evertsson, 2014).

For a particle with projected area A, local slip velocity u_r, gas density ρg, and drag coefficient C_D, a common magnitude representation is $F_D = 0.5\ C_D\ \rho g\ A\ |u_r|^2$. The effective gravitational force is $(\rho_p - \rho g)V_p g$. In a consistently defined rotating frame, centrifugal acceleration has magnitude $\omega^2 r$; the corresponding pseudo-force is not an additional force in the inertial-frame equation of motion. These representations are geometry-dependent idealizations, not a universal classifier model: drag closure and local flow fields must be chosen and validated for the geometry and concentration range (Johansson & Evertsson, 2012; Kim et al., 2020; Liu & Yu, 2025; Lu et al., 2021; Ren et al., 2023; Xing et al., 2015; Yu, 2018; Yu et al., 2014).

Figure 1 presents the competing influences without assigning a fixed d_{50}. The key distinction is between a theoretical equality of forces and an experimentally defined fifty-percent partition point, which integrates residence-time dispersion, short-circuiting, feed entry, and product collection.

For measured dry-solids streams, the size-class partition to coarse product is $P_{c,j} = (\dot{m}_c$

$f_{c,j})/(\dot{m}_F\ f_{F,j})$, where ṁ is dry-solids mass flow and f is the dry mass fraction in size class j.

All terms must refer to matching particle-size intervals. This definition is operational and should be distinguished from force-balance predictions.

For mineral/component k in size class j, the component-resolved partition to coarse is $P_{c,j,k} = (\dot{m}_c\ f_{c,j}\ x_{c,j,k})/(\dot{m}_F\ f_{F,j}\ x_{F,j,k})$, provided the class-component feed denominator is non-zero. Here $x_{s,j,k}$ is the measured mass fraction of component k in class j of stream s. This formulation is needed for beneficiation claims: a bulk partition curve alone cannot establish differential quartz, magnetite, hematite, or valuable-mineral recovery. All reported partition curves and

JIRRS
Journal International Review of Research Studies
Received: 13/06/2026 - **Accepted:** 13/11/2026
Vol: 1.11
DOI: 10.66104/gtgx0451
Pages: 1-32

comparative tables in this review use the destination label “partition to coarse”; a partition to fines is its complement only for a closed two-product class balance.

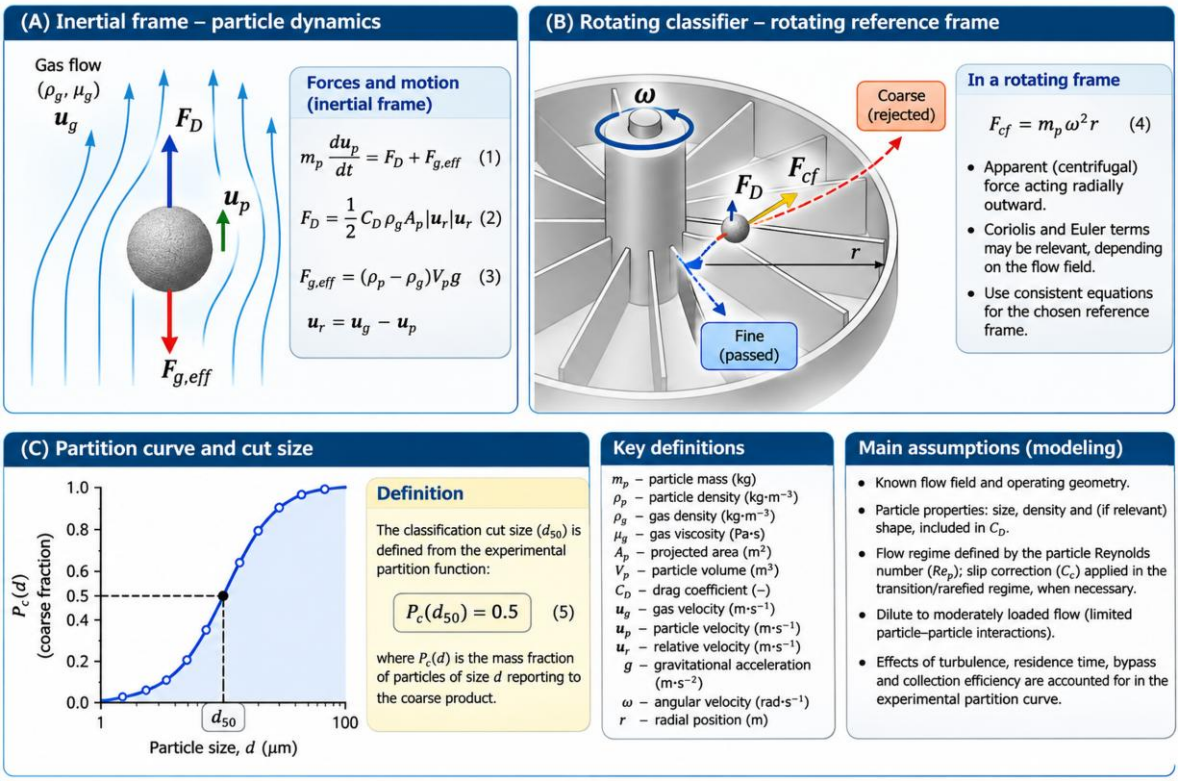

Figure 1. Conceptual force balance governing particle motion in air classifiers.
Note. Original conceptual illustration developed for this review with image-generation assistance; no experimental data are represented. All curves, labels, and equipment schematics are illustrative and do not establish measured performance. Disclosure remains subject to the journal’s image-generation policy.

This mechanistic basis explains why the same nominal particle size can report differently as mineral density changes. Classifier specifications should therefore use measured performance for the particular ore rather than transferring a generic rotor-speed–cut-size correlation.

4. Gravitational, Centrifugal, and Dynamic Rotor Classifiers

Gravitational and zigzag devices generate repeated opportunities for direction-dependent segregation and aerodynamic retention. Their apparent simplicity conceals interactions among feed presentation, stage geometry, cross-flow structure, and local solids concentration. Experimental grade-efficiency work is particularly valuable for distinguishing

JIRRS
Journal International Review of Research Studies
Received: 13/06/2026 - **Accepted:** 13/11/2026
Vol: 1.11
DOI: 10.66104/gtgx0451
Pages: 1-32

a true separative action from residence-time-dependent recirculation (Alade et al., 2025; Banjac et al., 2017; Denmud et al., 2019; Esmaeilpour et al., 2024; Hirajima et al., 2010; Ho et al., 2024a; Ho et al., 2025a; Ho et al., 2025b; Ho et al., 2024b; Hui et al., 2024).

Cyclonic and centrifugal equipment uses rotating gas motion to enhance radial transport. Geometry changes can alter vortex stability, turbulent dispersion, wall collection, and bypass; computational fluid dynamics (CFD) maps the internal flow field but does not establish industrial-grade efficiency. Model–experiment mismatch should be treated as evidence about unresolved turbulence, particle-wall interactions, or boundary conditions rather than removed by parameter tuning alone (Jayarathna et al., 2019; Kaas et al., 2024; Khoshdast et al., 2019; Koeninger et al., 2019; Lanzerstorfer, 2015; Li et al., 2016; Li et al., 2022a; Li et al., 2022b; Li & Yu, 2025; Lukas et al., 2020).

Dynamic rotor classifiers sharpen the practical trade-off between adjustable cut and flow resistance. Rotor cages, guide vanes, outlet arrangements, and secondary-air admission alter both local aerodynamic forces and residence-time distributions. Studies on quartz, cement, aggregates, coal, and analogous powders show technology-specific mechanisms; transferring a result between these materials requires normalization for density, shape, and feed-fines fraction (Mann et al., 2017; Mou et al., 2021; Pavlenko & Yukhymenko, 2026; Peng et al., 2024; Petit et al., 2018a; Petit & Irassar, 2024; Petit et al., 2018b; Petit et al., 2020; Ponomarev, 2025; Santos et al., 2024).

Figure 2 summarizes the three main technology categories. It is not a ranked scorecard: the nominally most controllable device may perform worse than a simple classifier when high fines loading creates agglomerates or when the product specification tolerates a wider distribution (Shin et al., 2026; Sun et al., 2019a; Sun et al., 2019b; Wrona et al., 2020; Yoshida et al., 2021; Yukhymenko et al., 2022; Toneva et al., 2011).

JIRRS
Journal International Review of Research Studies
Received: 13/06/2026 - **Accepted:** 13/11/2026
Vol: 1.11
DOI: 10.66104/gtgx0451
Pages: 1-32

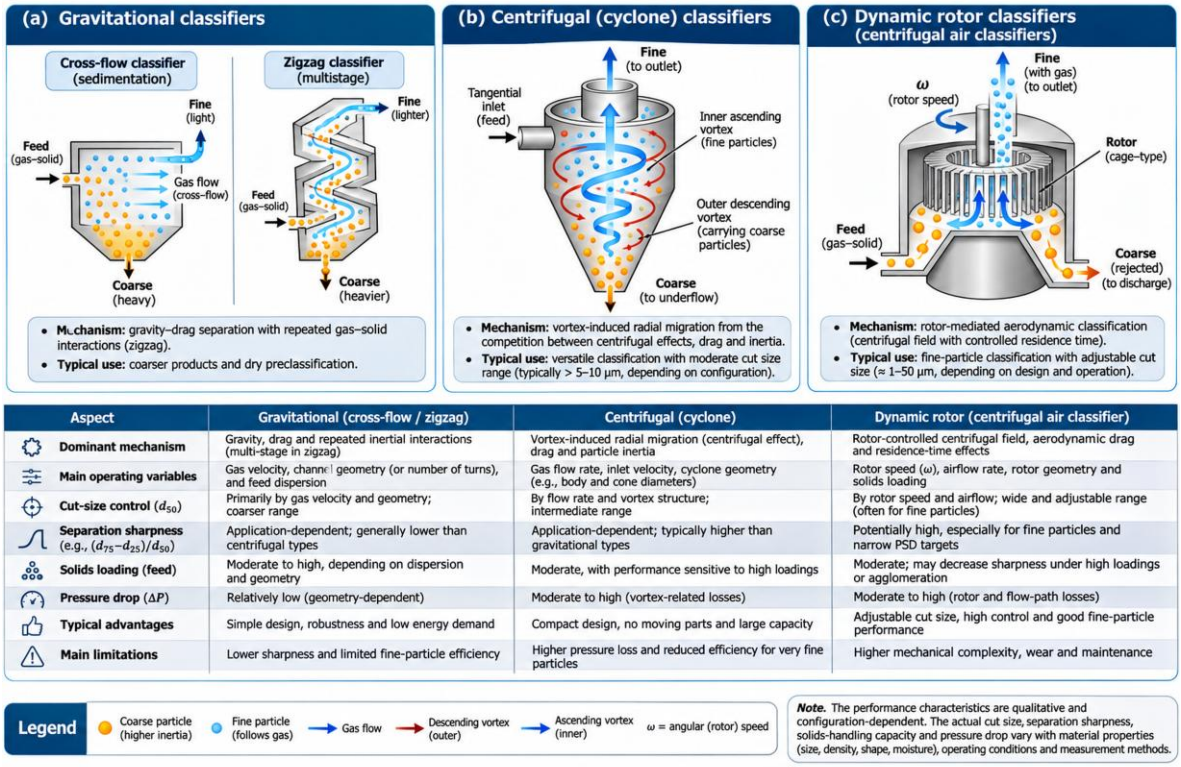

Figure 2. Technology-family map for gravitational, centrifugal, and dynamic rotor classification.
Note. Original conceptual illustration developed for this review with image-generation assistance; no experimental data are represented. All curves, labels, and equipment schematics are illustrative and do not establish measured performance. Disclosure remains subject to the journal's image-generation policy.

An illustrative reported case highlights the need to specify the operating context of separation metrics. Chan et al. (2026) compared several chamber-to-rotor diameter ratios in a vertical three-cage classifier. They reported a cut size of 22.4 µm and a sharpness indicator of 0.71 for the selected geometry. These are configuration-specific results and do not establish an operating envelope for other minerals or machines. The authors also compared calculated classification curves with experimental measurements, providing a stronger basis for interpreting the numerical predictions than geometry-only simulation. The available evidence should nevertheless be separated from broader claims of transferability to ore systems with different density distributions and surface properties.

The numerical sharpness indicator of 0.71 reported by Chan et al. (2026) should be interpreted only with that study's original mathematical definition; the present review does not

JIRRS
Journal International Review of Research Studies
Received: 13/06/2026 - **Accepted:** 13/11/2026
Vol: 1.11
DOI: 10.66104/gtgx0451
Pages: 1-32

identify it with imperfection I or use it for a cross-publication numerical ranking. Distinct reported sharpness and accuracy indices are not assumed equivalent.

Technology choice should begin with target product distributions and measured ore characteristics, then test controllability and pressure penalty. Direct ore evidence is more transferable than evidence from dissimilar powders, even if particle size matches.

5. Sharpness, Bypass, and Fish-Hook Behavior

Partition curves must state their destination convention: in this review, $P_c(d)$ denotes the mass fraction of a given size class reporting to the coarse product. The apparent cut $d_{50,app}$ satisfies $P_{c,obs}(d_{50,app}) = 0.5$. A bypass-corrected cut must be reported separately and cannot be conflated with this apparent value. Bypass and long tails mean the same d_{50} may coexist with very different fine contamination, and the use of imperfection or sharpness ratios is meaningful only after confirming consistent definitions (Abohelwa et al., 2023; Betz et al., 2021a; Betz et al., 2021b; Betz et al., 2022; Eswaraiah et al., 2012; Guizani et al., 2014; Kazys et al., 2021; Kundu et al., 2021).

For non-monotonic curves, d25, d50, and d75 are defined on the principal monotonic classification branch when multiple roots exist; otherwise, their extraction may be ambiguous. Imperfection is defined here as $I = (d75 - d25)/(2d50)$, with the apparent or corrected curve stated explicitly. When a genuinely size-independent coarseward bypass fraction b exists, and the remaining idealized partition has appropriate asymptotes, $P_{c,corr}(d) = [P_{c,obs}(d) - b]/(1 - b)$. This correction is not justified automatically for size-dependent bypass, appreciable fish-hook curvature, or incompatible end asymptotes; such data require a more suitable model or the uncorrected measured curve. Both apparent and corrected d50 should be reported where correction is supported.

Fish-hook behavior denotes a non-monotonic fine-size feature that can arise from particle–particle interactions, agglomeration, turbulent transport, or sampling and

JIRRS
Journal International Review of Research Studies
Received: 13/06/2026 - **Accepted:** 13/11/2026
Vol: 1.11
DOI: 10.66104/gtgx0451
Pages: 1-32

reconstruction error. A simulated hook does not prove its physical mechanism, especially if the feed-to-product material balance or sampling representativeness is unspecified. Experimental replication and reconciliation of feed, fine, and coarse fractions are necessary to distinguish a true phenomenon from biased data (Qian & Zeng, 2026; Sun et al., 2022; Tipici et al., 2024; Xie et al., 2025; Xie et al., 2026; Yan et al., 2024; Yang et al., 2023).

Figure 3 illustrates idealized and non-monotonic partition responses against particle size on a logarithmic micrometer scale. The plotted partition probability is dimensionless. These synthetic curves illustrate terminology, not experimentally obtained classifier performance or a universal bypass model.

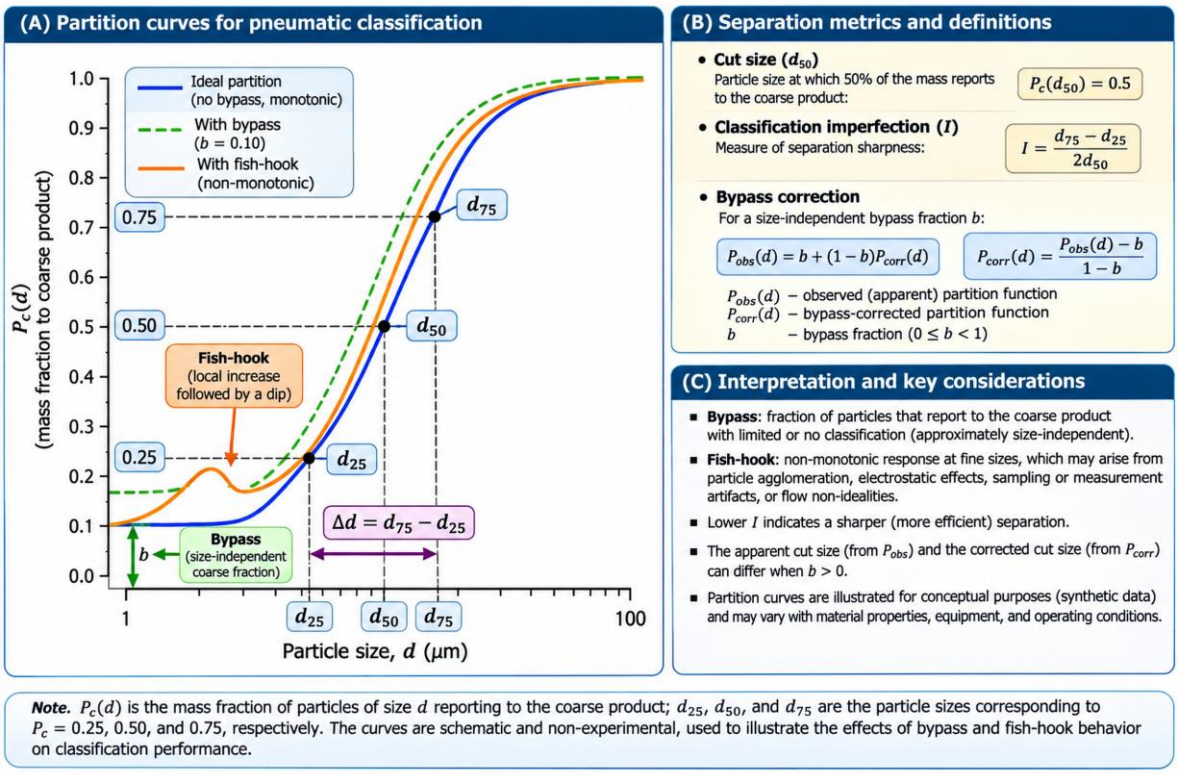

Figure 3. Illustrative coarse-product partition curves, with bypass and a fine-size fish-hook feature.
Note. Original conceptual illustration developed for this review with image-generation assistance; no experimental data are represented. All curves, labels, and equipment schematics are illustrative and do not establish measured performance. Disclosure remains subject to the journal's image-generation policy.

A reported fish-hook should be treated as an empirical feature of a measured grade-efficiency curve, not as a mechanism in itself. Betz et al. (2021a) modeled the phenomenon for

JIRRS
Journal International Review of Research Studies
Received: 13/06/2026 - **Accepted:** 13/11/2026
Vol: 1.11
DOI: 10.66104/gtgx0451
Pages: 1-32

centrifugal classification, while Eswaraiah et al. (2012) analyzed its appearance in a circulating air classifier. Comparing the two studies requires attention to curve definition, feed composition, solids loading, and how they sampled very fine fractions. Without those controls, apparent agreement in curve shape cannot be interpreted as evidence of identical particle trajectories.

A sharp central partition transition does not ensure a clean coarse product when fine-particle bypass is appreciable. Meaningful reporting requires the partition convention and, where justified by the data, d_{25}, d_{50}, d_{75}, a bypass estimate, component recoveries, and uncertainty intervals. An imperfection index such as $(d_{75} - d_{25})/(2d_{50})$ is comparable across studies only when the same corrected or uncorrected curve convention is used.

Where independent replicate data are available, the fitted cut must be reported as d50 ± u(d50) or with a confidence interval obtained by replicate fits, bootstrap resampling, or uncertainty propagation. Differences between two nominal cuts must not be interpreted as meaningful without such uncertainty. For any numerical sharpness comparison, the full defining equation and the reference curve (observed or bypass-corrected) must accompany the estimate.

6. Airflow, Rotor Speed, Solids Loading, and Pressure Losses

Airflow controls both aerodynamic transport and turbulence, whereas rotor speed adjusts the competing inertial environment in dynamic systems. Their effects are coupled: changing one often alters internal pressure distribution, feed dispersion, and apparent cut. Solids loading adds another state variable through collisions, flow obstruction, and localized particle concentration. Operating maps should therefore be multivariate rather than single-factor charts (Cao et al., 2024; Chan et al., 2026; Feng et al., 2018; Huang et al., 2024a; Huang et al., 2023; Huang et al., 2024b; Li et al., 2024; Li et al., 2025a; Li et al., 2025b).

Solids loading must be defined on a declared basis, e.g., $\Lambda = \dot{m}_s/\dot{m}_g$ (dry-solids-to-gas mass-flow ratio) or $L_V = \dot{m}_s/Q_g$ (mass per actual gas volume). State whether gas volumes are actual, standard, or normal, with the temperature/pressure basis. Rotor rotational speed by itself is not a transferable severity variable without geometry, gas rate, and loading.

JIRRS
Journal International Review of Research Studies
Received: 13/06/2026 - **Accepted:** 13/11/2026
Vol: 1.11
DOI: 10.66104/gtgx0451
Pages: 1-32

Pressure drop is a hydraulic burden, not itself an electrical energy-consumption metric. Fan efficiency, rotor drive, pneumatic transport, dust collection, and auxiliary handling establish the actual boundary. Comparisons that report only classifier differential pressure or only mill motor power cannot support claims about total circuit specific energy (Liu et al., 2015; Otwinowski et al., 2022; Peng et al., 2022; Ren et al., 2016a; Ren et al., 2016b; Sun et al., 2021a; Sun et al., 2021b; Sun et al., 2017; Wang et al., 2025).

A consistent electrical-energy boundary may be expressed as $SEC_{class} = [(\Delta P\ Q_g/\eta_{fan}) + P_{rotor} + P_{aux}]/\dot{m}_{s,dry}$, with all numerator terms in kW and dry-solids throughput in t/h to obtain kWh/t_{dry} solids; Q_g is actual volumetric flow (m^3/s), ΔP is Pa, and $\Delta P\ Q_g$ is converted from W to kW. The chosen boundary must identify fan, rotor, pneumatic conveying, dust collection, deagglomeration, and auxiliary handling without double counting. State pressure tap locations (static versus total), gas temperature, density and flow rate. Classifier-only and whole-circuit SEC values are not interchangeable.

Flow stabilization with baffles, guide cones, volute and vortex-finder adjustments, or secondary air can reduce unwanted recirculation, but may also create additional pressure losses or sensitivity to feed distribution. Predictive data-driven models can summarize trained operating states; extrapolation outside the calibration envelope requires validation, especially under changing mineral density or moisture (Wu et al., 2017; Wu et al., 2016; Yu et al., 2020; Yu et al., 2023a; Yu et al., 2023b; Yu et al., 2024a; Yu et al., 2019; Yuan et al., 2024; Zeng et al., 2022).

For industrial selection, the priority is repeatable quality across the operating window rather than a single optimum at clean, low-loading laboratory conditions. Investigations of multistage and multi-product designs should explicitly identify whether apparent gains are due to altered product recoveries or simply different cut definitions (Zeng et al., 2020; Zhao et al., 2018; Zhao et al., 2024; Zhou & Shen, 2022; Zhou et al., 2024; Zhu et al., 2024; Zinurov et al., 2022).

JIRRS
Journal International Review of Research Studies
Received: 13/06/2026 - **Accepted:** 13/11/2026
Vol: 1.11
DOI: 10.66104/gtgx0451
Pages: 1-32

7. Particle Density, Shape, Moisture, and Agglomeration

A classifier is intrinsically sensitive to aerodynamic equivalence, not mineral identity. Two particles of similar sieve diameter may follow different trajectories because their densities, aspect ratios, roughness, and dynamic drag differ. Blended feeds can therefore exhibit component-specific partition curves and a misleading single bulk d_{50}. Mineral liberation and composition-resolved mass balances are central when separation is used as beneficiation rather than solely for size control (Abohelwa et al., 2024; Alade et al., 2025; Altun, 2022; Altun et al., 2016; Cao et al., 2024; Cepuritis et al., 2015; Hirajima et al., 2010; Kaas et al., 2024; Kim et al., 2020).

For shape-sensitive comparisons, report the PSD size basis and, where available, aspect ratio, circularity, and sphericity or an appropriate shape factor. Geometric sieve size and operational aerodynamic size are not equivalent. For cohesive fines distinguish primary-particle size from aerodynamic agglomerate size and document moisture by mass, ambient relative humidity, conditioning protocol and equilibration interval. Size control aims at a product PSD; dry beneficiation additionally requires chemical/mineralogical assays and component-specific recovery.

Moisture can increase adhesion and agglomerate formation, perturbing both the fine-particle cut and the reliability of dry laser diffraction or sieve PSD results. Feed conditioning, sample disaggregation, and humidity control need to be reported explicitly. Results from coal ash, manufactured sand, fine powders, and recycled materials offer informative process analogies but should not be presented as equivalent ore-specific measurements (Koeninger et al., 2019; Liu & Yu, 2024; Liu et al., 2024a; Pereira, 2026a; Petit et al., 2018a; Petit & Irassar, 2021; Ponomarev, 2025; Ren et al., 2023).

Table 2 summarizes plausible mechanisms through which feed properties influence measured separation; it does not assert universal signs or magnitudes of response. The strongest test is component-resolved classification in which chemical or mineralogical phase distributions are measured for each product (Shin et al., 2026; Wockenfuss et al., 2023; Wrona et al., 2020; Yu et al., 2025; Yu et al., 2024a).

JIRRS
Journal International Review of Research Studies
Received: 13/06/2026 - **Accepted:** 13/11/2026
Vol: 1.11
DOI: 10.66104/gtgx0451
Pages: 1-32

Table 2.Material attributes affecting pneumatic classification and interpretation.

Attribute	Likely mechanism	Necessary measurement	Interpretive caution
Mineral density	Altered inertial/gravitational response	Phase density and component assay	Bulk d_{50} hides differential partition
Particle shape	Projected area / orientation-dependent drag	Microscopy or dynamic shape index	Sieve size differs from aerodynamic size
Moisture	Adhesion, cohesive clumps	Moisture and ambient RH	Apparent coarse tail may be agglomeration
Fines fraction	Crowding and entrainment	Full feed PSD and throughput	Loading shifts observed cut
Feed blending	Component interaction	Separate component grade curves	Single-component tests may mislead

Note. Qualitative mechanism-based synthesis; effect signs and magnitude must be validated for each material and operating regime.

Consequently, equipment comparisons made without ore-density distribution, particle shape, moisture, and feed-size characterization may confound changes in classifier design with differences in aerodynamic feed response.

8. Measuring Partition Curves and Sampling Bias

A defensible partition curve requires independently representative feed, fine-product, and coarse-product samples, each paired with dry-solids mass flows and compatible size distributions collected over a stable operating interval. Where direct measurement is difficult, reconciliation techniques must document assumptions and propagated error. Dust carryover and size-dependent sampling losses can deform the fine end of the partition curve, potentially creating or exaggerating an apparent fish-hook (Barimani et al., 2018; Eswaraiah et al., 2019; Huang et al., 2024a; Kazys et al., 2021; Kundu et al., 2021; Liu et al., 2024a; Lukas et al., 2020).

Sampling at the classifier inlet and the coarse/fine outlets is complicated by anisokinetic extraction, nonuniform spatial concentration, deposits in sampling lines, and transient feed fluctuations. Repeated isokinetic (or otherwise justified) protocols and independent recovery checks should be preferred over one-off grab samples. Figure 4 gives an auditable sequence from sampling to uncertainty analysis (Mann et al., 2017; Roloff et al., 2019; Tipici et al., 2024; Xie et al., 2025; Xing et al., 2015; Yan et al., 2024).

JIRRS
Journal International Review of Research Studies
Received: 13/06/2026 - **Accepted:** 13/11/2026
Vol: 1.11
DOI: 10.66104/gtgx0451
Pages: 1-32

Where gas–solid duct extraction is required, document sampling-port and traverse locations, nozzle orientation and dimensions, duct gas velocity, extraction velocity, sampling duration and stability window; use isokinetic extraction where applicable or quantify the deviation. Replicate, time-integrated measurements are preferable to grab samples in fluctuating systems. Feed and product PSD analyses must use the same or validated-equivalent dispersion and sizing basis, including refractive-index assumptions and agglomerate disaggregation.

A generalized dry-solids balance is $\dot{m}_F = \dot{m}_c + \dot{m}_f + \dot{m}_{dust/loss} + dM_{inventory}/dt$. At steady state the accumulation is approximately zero. Bag-filter or cyclone solids are counted within fine product only where the explicitly defined fine-product boundary includes them. For a closed two-product boundary, the class balance is $\dot{m}_F\, f_{F,j} \approx \dot{m}_f\, f_{f,j} + \dot{m}_c\, f_{c,j}$; its signed closure residual is $\varepsilon_j\,(\%) = 100[\dot{m}_f\, f_{f,j} + \dot{m}_c\, f_{c,j} - \dot{m}_F\, f_{F,j}]/(\dot{m}_F\, f_{F,j})$, provided the denominator is positive. Where dust/loss is a separate measured stream, its classwise contribution must also enter the numerator. The size-class partition is interpretable only if these balances are sufficiently reconciled for the stated sampling and measurement uncertainty. A monotonic curve fit should not be imposed on a demonstrably non-monotonic set of measured size-class recoveries.

JIRRS
Journal International Review of Research Studies
Received: 13/06/2026 - **Accepted:** 13/11/2026
Vol: 1.11
DOI: 10.66104/gtgx0451
Pages: 1-32

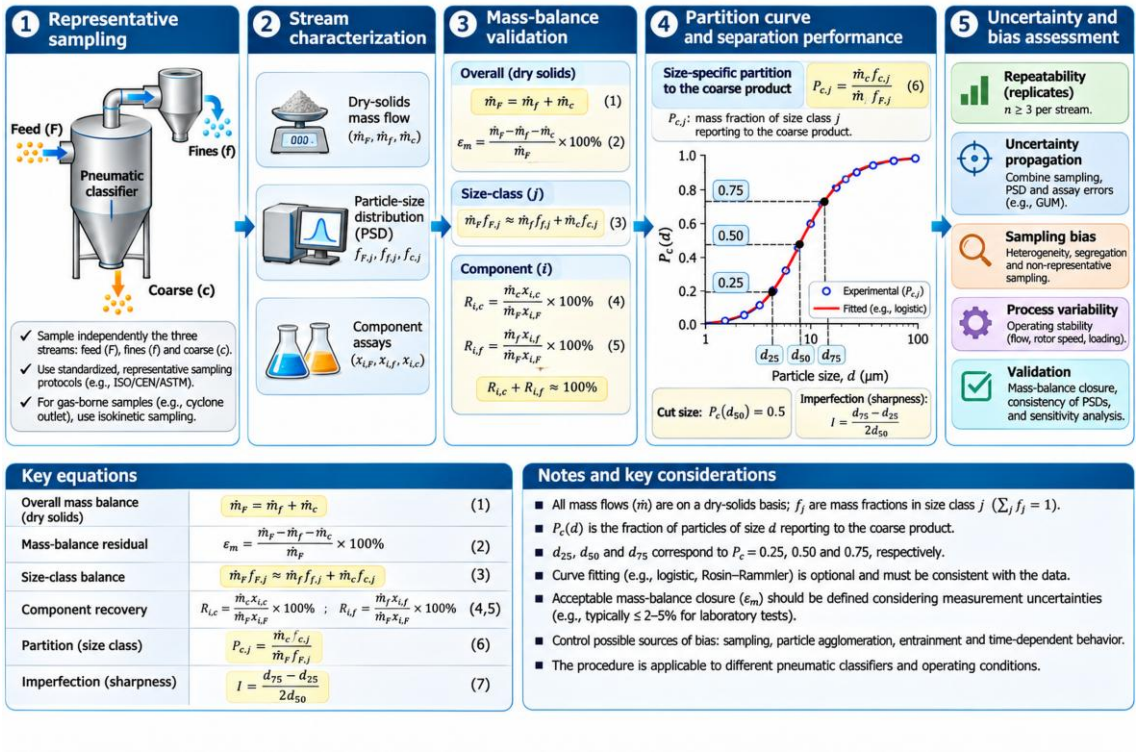

Figure 4. Minimum experimental sequence for reproducible classifier grade-efficiency assessment.
Note. Original conceptual illustration developed for this review with image-generation assistance; no experimental data are represented. All curves, labels, and equipment schematics are illustrative and do not establish measured performance. Disclosure remains subject to the journal's image-generation policy.

Table 3 identifies the essential measurements and why each matters. The most serious reporting weakness is often not a missing derived parameter, but the absence of sufficient raw observations to recompute and independently check it.

Table 3.Minimum dataset and checks for reproducible classifier performance measurement.

Element	Minimum reported data	Reason for inclusion
Mass balance	Feed, coarse, fines rates and closure	Detect bypass and sampling errors
Particle sizing	PSD by comparable method for each stream	Compute size-wise distribution
Grade efficiency	$P_c(d)$ (partition to coarse), d_{25}, d_{50}, d_{75}	Assess sharpness and fine carryover
Feed properties	Density, shape, moisture, mineral chemistry	Control aerodynamic confounding
Operating state	Airflow, pressure drop, speed, loading	Compare equivalent conditions
Uncertainty	Replicates, intervals, PSD method bias	Prevent overinterpretation

JIRRS
Journal International Review of Research Studies
Received: 13/06/2026 - **Accepted:** 13/11/2026
Vol: 1.11
DOI: 10.66104/gtgx0451
Pages: 1-32

Note. The listed measurements are recommended reporting requirements, not claims that all cited studies supplied these items.

Before classifiers are benchmarked, report overall dry-solids closure and size-class reconciliation, the number of independent replicates, and uncertainty in the inferred partition curve. Where simulations supply an unmeasured response, label the curve as predicted; a computed curve is not independent experimental validation.

A modeled CFD/DEM or data-driven curve must disclose turbulence closure, drag law, particle–wall interactions, solids loading and coupling assumptions, mesh independence, calibration data, and independently held-out validation data. Model calibration is parameter fitting; comparison against those same calibration observations is not independent validation. External transfer tests should challenge feed PSD, mineral density, moisture, geometry, and loading, particularly for neural-network pressure predictions.

9. Technology Benchmarking and Research Gaps

Technology benchmarking requires a common feed characterization and a common product objective. A useful comparison tests the same mineral feed in competing classifier families at matched target d_{50}, and then compares sharpness, coarse contamination, capacity, pressure loss, stability, and product recovery. Laboratory cross-comparisons, plant characterization, and industrial feasibility reviews answer different questions and should be stratified accordingly (Ansari et al., 2025; Esmaeilpour et al., 2024; Fu et al., 2024; Huang et al., 2026; Jia et al., 2021; Kaas et al., 2022; Kundu et al., 2021; Li et al., 2016).

In a matched-duty benchmark, each device should first be optimized independently for an agreed product requirement or cut on the same characterized feed. Comparison should then report identical coarse-partition convention, d25/d50/d75 and imperfection definition, observed bypass, component recovery (where applicable), dry-solids throughput, SEC under a declared boundary, operating stability and uncertainty. Evidence from industrial mineral units (class A) receives greater transfer weight than non-mineral analogs (class D), without assuming all field measurements are intrinsically unbiased.

Benchmarking is impeded by proprietary geometry, missing feed component assays, inconsistent bypass correction, and diverse definitions of specific energy. Existing work on

JIRRS
Journal International Review of Research Studies
Received: 13/06/2026 - **Accepted:** 13/11/2026
Vol: 1.11
DOI: 10.66104/gtgx0451
Pages: 1-32

prediction, optimization, and industrial scale-up can guide test planning but cannot establish a universal classifier ranking. The priority research gap is cross-technology testing with open partition data and sufficient replication to quantify loading-by-density interactions (Mou et al., 2021; Pereira, 2026a; Pereira, 2026b; Pukkella et al., 2023; Santos et al., 2024; Vokurka et al., 2025; Yoshida et al., 2021; Yu et al., 2025).

A defensible comparison table would state the same feed mineralogy, feed-size distribution, solids loading, dry-air conditions, separator geometry, partition convention, power-accounting boundary, and confidence limits for each technology. Absent those controls, a ranking by d_{50} or pressure drop alone is not evidence of superior industrial performance.

10. Cross-Study Critical Discussion and Limitations

Comparing the smallest reported cut sizes across equipment designs is misleading when the feeds, flow rates, and partition conventions differ. In practice, the observable cut is a conditional statistic of apparatus, feed, loading, and measurement method. Separating these determinants gives a stronger basis for selecting a classifier than ranking publications by their finest reported cut. Nor does increasingly complex CFD or machine learning guarantee accuracy if independent experiments do not confirm their predictions.

Three limitations constrain this synthesis. First, the supplied database is not an independently screened, complete corpus; therefore, citation counts cannot be interpreted as publication prevalence or meta-analytic weights. Second, much of the methodological evidence transfers from non-mineral powders, which is useful for fluid mechanics but not direct proof of mineral separation performance. Third, full-text verification of every included item and DOI has not been completed in this drafting pass. Accordingly, numeric operating envelopes and cross-study averaged effect sizes are intentionally withheld.

A practical evidence ladder is recommended: validate physical feed properties; collect closed mass balances and partition curves at multiple operating points; compare against simulation only after holding out independent data; and report pilot-to-industrial shifts as mechanism changes rather than solely changes in nominal throughput. This avoids overstating technical readiness or transferability of one laboratory optimum.

JIRRS
Journal International Review of Research Studies
Received: 13/06/2026 - **Accepted:** 13/11/2026
Vol: 1.11
DOI: 10.66104/gtgx0451
Pages: 1-32

11. Conclusions and Recommendations

The technical value of a pneumatic classifier depends on the separation it achieves for a specified feed under reproducible operating conditions and a transparent measurement protocol. A median cut size is insufficient to characterize selectivity: bypass, partition sharpness, component recovery, pressure losses, and operating stability jointly determine a classifier's suitability for a specified feed and product. Rotor classifiers provide an adjustable separation mechanism, while gravity-based and cyclone-based alternatives may better match duties where coarser separation, simplicity, or throughput matters more than a narrow cut.

Future industrial studies should pair component-resolved mineral characterization with replicated partition curves and explicit mass-balance reconciliation. They should investigate density and shape effects, moisture-induced agglomeration, and high-loading bypass under equivalent operating boundaries. The proposed benchmarking protocol prioritizes matched feeds, uncertainty reporting, and cross-scale validation.

Declarations

Funding

This review received no specific external funding.

Conflict of Interest

The author declares no conflict of interest.

Data Availability

No new experimental datasets were generated. All quantitative values discussed in the review are traceable to the cited literature.

Author Contributions

The author performed conceptualization, critical analysis, literature synthesis, visualization, and manuscript preparation.

References

Abohelwa, M., Benker, B., Javadi, M., Wollmann, A., & Weber, A. P. (2023). Limitations in the performance of fine powder separation in a turbo air classifier. Processes, 11(10), 2817. https://doi.org/10.3390/pr11102817

JIRRS
Journal International Review of Research Studies

Received: 13/06/2026 - **Accepted:** 13/11/2026
Vol: 1.11
DOI: 10.66104/gtgx0451
Pages: 1-32

Abohelwa, M., Wollmann, A., Benker, B., Plack, A., Javadi, M., & Weber, A. P. (2024). Size classification and material sorting of fine powders with a deflector wheel air classifier and an electrostatic separator. Powders, 3(4), 550–573. https://doi.org/10.3390/powders3040029

Alade, J., Eterigho-Ikelegbe, O., & Bada, S. (2025). Optimized design and fabrication of a wind-sifter separator for enhanced dry beneficiation of high-ash coal. Fuel, 386, 134230. https://doi.org/10.1016/j.fuel.2024.134230

Altun, O. (2022). Air classification performances of the components within the varied feed blends. Powder Technology, 399, 117092. https://doi.org/10.1016/j.powtec.2021.117092

Altun, O., & Benzer, H. (2014). Selection and mathematical modeling of high-efficiency air classifiers. Powder Technology, 264, 1–8. https://doi.org/10.1016/j.powtec.2014.05.013

Altun, O., Toprak, A., Benzer, H., & Darilmaz, O. (2016). Multi-component modeling of an air classifier. Minerals Engineering, 93, 50–56. https://doi.org/10.1016/j.mineng.2016.04.014

Ansari, M., Khademi, P., Pourkhosravani, A., Ghasemi, A., Karbakhsh, V., & Banisi, S. (2025). Characterization and performance analysis of the dynamic air separator of the GoleGohar pelletizing plant. Minerals Engineering, 227, 109260. https://doi.org/10.1016/j.mineng.2025.109260

Bagherzadeh, A., Darbandi, M., & Barezban, M. B. (2024). Numerical simulation of particle separation in a two-phase flow passing through a vortex-based air classifier using an Eulerian–Lagrangian DDPM approach. Powder Technology, 445, 120036. https://doi.org/10.1016/j.powtec.2024.120036

Banjac, V., Pezo, L., Pezo, M., Vukmirović, Đ., Čolović, D., Fišteš, A., & Čolović, R. (2017). Optimization of the classification process in the zigzag air classifier for obtaining a high-protein sunflower meal – Chemometric and CFD approach. Advanced Powder Technology, 28(3), 1069–1078. https://doi.org/10.1016/j.apt.2017.01.013

Barimani, M., Green, S., & Rogak, S. (2018). Particulate concentration distribution in centrifugal air classifiers. Minerals Engineering, 126, 44–51. https://doi.org/10.1016/j.mineng.2018.06.007

Betz, M., Gleiss, M., & Nirschl, H. (2021a). Effects of flow baffles on flow profile, pressure drop and classification performance in classifiers. Processes, 9(7), 1213. https://doi.org/10.3390/pr9071213

Betz, M., Nirschl, H., & Gleiss, M. (2021b). Development of a new solver to model the fish-hook effect in a centrifugal classifier. Minerals, 11(7), 663. https://doi.org/10.3390/min11070663

JIRRS
Journal International Review of Research Studies
Received: 13/06/2026 - **Accepted:** 13/11/2026
Vol: 1.11
DOI: 10.66104/gtgx0451
Pages: 1-32

Betz, M., Nirschl, H., & Gleiss, M. (2022). Development of prediction models for pressure loss and classification efficiency in classifiers. Processes, 10(4), 627. https://doi.org/10.3390/pr10040627

Caliskan, M. E., Karagoz, I., Avci, A., & Surmen, A. (2019). Investigation into the effects of various parameters on the performance and classification potential of a cyclone classifier. Powder Technology, 356, 102–111. https://doi.org/10.1016/j.powtec.2019.07.104

Cao, Y., Li, X., Jiao, Z., Liu, J., Yang, W., & Yu, Y. (2024). Powder agglomeration characterization of pneumatic classification and the factors influencing agglomeration. Journal of Beijing University of Chemical Technology, 51(3), 66–75. https://doi.org/10.13543/j.bhxbzr.2024.03.007

Cepuritis, R., Jacobsen, S., & Onnela, T. (2015). Sand production with VSI crushing and air classification: Optimizing fines grading for concrete production with micro-proportioning. Minerals Engineering, 78, 1–14. https://doi.org/10.1016/j.mineng.2015.03.025

Chan, Q., Wang, F., Liu, H., & Fang, Y. (2026). The effect of classifier chamber configuration on flow field and performance in vertical three-cage classifiers. Processes, 14(12), 1992. https://doi.org/10.3390/pr14121992

Denmud, N., Baite, K., Plookphol, T., & Janudom, S. (2019). Effects of operating parameters on the cut size of turbo air classifier for particle size classification of SAC305 lead-free solder powder. Processes, 7(7), 427. https://doi.org/10.3390/pr7070427

Esmaeilpour, M., Mohebbi, A., & Ghalandari, V. (2024). CFD simulation and optimization of an industrial cement gas–solid air classifier. Particuology, 89, 172–184. https://doi.org/10.1016/j.partic.2023.10.011

Eswaraiah, C., Angadi, S. I., & Mishra, B. K. (2012). Mechanism of particle separation and analysis of fish-hook phenomenon in a circulating air classifier. Powder Technology, 218, 57–63. https://doi.org/10.1016/j.powtec.2011.11.036

Eswaraiah, C., Soni, R. K., Tripathy, S. K., & Filippov, L. O. (2019). Particle classification optimization of a circulating air classifier. Mineral Processing and Extractive Metallurgy Review, 40(5), 314–322. https://doi.org/10.1080/08827508.2019.1643340

Feng, L., Wu, Y., Wang, J., & Zhang, H. (2018). Prediction model for cut size in turbo air classifiers. Chemical Industry and Engineering Progress, 37(12), 4579–4585. https://doi.org/10.16085/j.issn.1000-6613.2018-0366

Fu, M., Cao, Z., Chen, X., Gao, Z., & Zhan, M. (2024). Research progress of air classification technology and equipment. Chemical Industry and Engineering, 41(4), 117–130. https://doi.org/10.13353/j.issn.1004.9533.20230510

Fu, P., Wang, F., Ma, L., Yang, X., & Wang, H. (2016). Fine particle sorting and classification in the cyclonic centrifugal field. Separation and Purification Technology, 158, 357–366. https://doi.org/10.1016/j.seppur.2015.12.044

JIRRS
Journal International Review of Research Studies
Received: 13/06/2026 - **Accepted:** 13/11/2026
Vol: 1.11
DOI: 10.66104/gtgx0451
Pages: 1-32

Gao, L., Yu, Y., & Liu, J. (2013). Study on the cut size of a turbo air classifier. Powder Technology, 237, 520–528. https://doi.org/10.1016/j.powtec.2012.12.043

Guizani, R., Mokni, I., Mhiri, H., & Bournot, P. (2014). CFD modeling and analysis of the fish-hook effect on the rotor separator's efficiency. Powder Technology, 264, 149–157. https://doi.org/10.1016/j.powtec.2014.05.020

Hirajima, T., Petrus, H. T. B. M., Oosako, Y., Nonaka, M., Sasaki, K., & Ando, T. (2010). Recovery of cenospheres from coal fly ash using a dry separation process: Separation estimation and potential application. International Journal of Mineral Processing, 95(1–4), 18–24. https://doi.org/10.1016/j.minpro.2010.03.004

Ho, N. X., Dinh, H. T., & Dau, N. T. (2024a). The effects of the guide cone on the flow field and key classification performance of an industrial-scale micron air classifier. Applied Sciences, 14(24), 11504. https://doi.org/10.3390/app142411504

Ho, N. X., Dinh, H. T., & Dau, N. T. (2025a). Numerical study to optimize the operating parameters of a real-sized industrial-scale micron air classifier used for manufacturing fine quartz powder and a comparison with the prototype model. Processes, 13(1), 106. https://doi.org/10.3390/pr13010106

Ho, N. X., Dinh, H. T., & Dau, N. T. (2025b). Effects of the rotor speed on the flow field and classification performance of an industrial-scale micron air classifier using a two-way coupled CFD-DPM model. Lecture Notes in Mechanical Engineering, 341–348. https://doi.org/10.1007/978-3-031-96122-9_41

Ho, N. X., Dinh, H. T., Dau, N. T., & Nguyen, B. H. (2024b). A numerical study on the flow field and classification performance of an industrial-scale micron air classifier under various outlet mass airflow rates. Processes, 12(9), 2035. https://doi.org/10.3390/pr12092035

Huang, L., Li, W., Liu, R., Yuan, J., Li, X., Jiang, H., & Duan, C. (2024a). Dynamic characteristics of the internal flow field of a rotary centrifugal air classifier and pressure prediction through attention mechanism-enhanced CNN-LSTM. Advanced Powder Technology, 35(8), 104578. https://doi.org/10.1016/j.apt.2024.104578

Huang, L., Li, W., Liu, R., Zhang, Y., Pan, M., Zhao, Y., Jiang, H., & Duan, C. (2024b). Experimental study of multiscale dynamic characterization of the gas-solid phase in a disturbing rotary centrifugal air classifier using pressure signal testing and analysis methods. Powder Technology, 443, 119926. https://doi.org/10.1016/j.powtec.2024.119926

Huang, L., Liu, R., Huang, F., Yuan, J., Wen, D., Liu, Q., Zhao, Y., Jiang, H., & Kuang, S. (2023). Study on classifying particle size and spatial internal flow field of T-shaped tooth structure in a disturbing rotary centrifugal air classifier. Advanced Powder Technology, 34(11), 104230. https://doi.org/10.1016/j.apt.2023.104230

JIRRS
Journal International Review of Research Studies
Received: 13/06/2026 - **Accepted:** 13/11/2026
Vol: 1.11
DOI: 10.66104/gtgx0451
Pages: 1-32

Huang, L., Liu, R., Miao, Q., Zou, R., Jiang, H., & Duan, C. (2024c). Dynamic characterization of the flow field of air classifier disturbed structures and application to efficient separation of fly ash. Journal of Environmental Chemical Engineering, 12(6), 114706. https://doi.org/10.1016/j.jece.2024.114706

Huang, L., Yuan, J., Liu, R., Zhang, Y., Jiang, H., & Wang, H. (2026). Research progress on performance evaluation and optimization methods of air classifiers. Minerals Engineering, 248, 110590. https://doi.org/10.1016/j.mineng.2026.110590

Huang, Q., Liu, J., & Yu, Y. (2012). Turbo air classifier guide vane improvement and inner flow field numerical simulation. Powder Technology, 226, 10–15. https://doi.org/10.1016/j.powtec.2012.03.026

Hui, C., Li, Q., Peng, J., & Fang, Y. (2024). Computational fluid dynamics simulation and performance study of a three-separation combined air classifier. Thermal Science, 28(2C), 1589–1603. https://doi.org/10.2298/TSCI230513183H

Jayarathna, C. K., Balfe, M., Moldestad, B. M. E., & Tokheim, L.-A. (2019). Improved multi-stage cross-flow fluidized bed classifier. Powder Technology, 342, 621–629. https://doi.org/10.1016/j.powtec.2018.10.026

Jia, F., Mou, X., Fang, Y., & Chen, C. (2021). A new rotor-type dynamic classifier: Structural optimization and industrial applications. Processes, 9(6), 1033. https://doi.org/10.3390/pr9061033

Johansson, R., & Evertsson, M. (2014). CFD simulation of a centrifugal air classifier used in the aggregate industry. Minerals Engineering, 63, 149–156. https://doi.org/10.1016/j.mineng.2014.03.013

Johansson, R., & Evertsson, M. (2012). CFD simulation of a gravitational air classifier. Minerals Engineering, 33, 20–26. https://doi.org/10.1016/j.mineng.2012.01.007

Kaas, A., Mütze, T., & Peuker, U. A. (2022). Review on zigzag air classifier. Processes, 10(4), 764. https://doi.org/10.3390/pr10040764

Kaas, A., Wilke, C., Rabaschus, J.-S., Mütze, T., & Peuker, U. A. (2024). Modeling the sorting of lithium-ion battery components in a zig-zag air classifier. Metals, 14(3), 269. https://doi.org/10.3390/met14030269

Kazys, R., Sliteris, R., Mazeika, L., Van den Abeele, L., Nielsen, P., & Snellings, R. (2021). Ultrasonic monitoring of variations in dust concentration in a powder classifier. Powder Technology. https://doi.org/10.1016/j.powtec.2020.11.072

Khoshdast, H., Soflaeian, A., & Shojaei, V. (2019). Coupled fuzzy logic and experimental design application for simulation of a coal classifier in an industrial environment. Physicochemical Problems of Mineral Processing, 55(2). https://doi.org/10.5277/ppmp18161

Kim, M., Cha, J., & Go, J. S. (2020). Ring-shaped baffle effect on separation performance of lithium carbonate microparticles in a centrifugal classifier. Micromachines, 11(11), 980. https://doi.org/10.3390/mi11110980

JIRRS
Journal International Review of Research Studies
Received: 13/06/2026 - **Accepted:** 13/11/2026
Vol: 1.11
DOI: 10.66104/gtgx0451
Pages: 1-32

Koeninger, B., Spoetter, C., Romeis, S., Weber, A. P., & Wirth, K.-E. (2019). Classifier performance during dynamic fine grinding in fluidized-bed opposed-jet mills. Advanced Powder Technology, 30(8), 1678–1686. https://doi.org/10.1016/j.apt.2019.05.018

Kundu, T., Das, S. K., Tripathy, S. K., & Angadi, S. I. (2021). Performance evaluation of the VSK separator for treating mineral fines. Minerals Engineering, 167, 106883. https://doi.org/10.1016/j.mineng.2021.106883

Lanzerstorfer, C. (2015). Application of air classification for improved recycling of sinter plant dust. Resources, Conservation and Recycling, 94, 66–71. https://doi.org/10.1016/j.resconrec.2014.11.013

Li, H., He, Y., Shi, F., Zuo, W., Zhou, N., Wei, H., Wang, S., & Xie, W. (2016). Performance of the static air classifier in a vertical spindle mill. Fuel, 177, 8–14. https://doi.org/10.1016/j.fuel.2016.02.090

Li, H., Song, Z., Sun, Z., Zhang, A., Si, H., Hu, R., Yang, C., Zhang, S., & Jin, L. (2022a). Operational performance characteristics of an axial double-baffle three-channel classifier for coarse pulverized coal. Powder Technology, 400, 117250. https://doi.org/10.1016/j.powtec.2022.117250

Li, Q., Mou, X., & Fang, Y. (2022b). Effects of a guide cone on the flow field and performance of a new dynamic air classifier. Processes, 10(5), 874. https://doi.org/10.3390/pr10050874

Li, W., Li, X., Yuan, J., Liu, R., Liu, Y., Ye, Q., Jiang, H., & Huang, L. (2024). Pressure prediction for air cyclone centrifugal classifier based on CNN-LSTM enhanced by attention mechanism. Chemical Engineering Research and Design, 205, 775–791. https://doi.org/10.1016/j.cherd.2024.04.045

Li, W., Liu, Y., Liu, R., Yang, Y., Duan, C., Huang, L., & Jiang, H. (2025a). A hybrid EMD-GRU model for pressure prediction in air cyclone centrifugal classifiers. Advanced Powder Technology, 36(1), 104743. https://doi.org/10.1016/j.apt.2024.104743

Li, X., & Yu, Y. (2025b). Design and study of a dual-layer rotor cage for ultrafine powder classification. CIESC Journal, 76(12), 6328–6338. https://doi.org/10.11949/0438-1157.20250653

Li, X., Liu, R., Liu, Y., Yuan, J., Duan, C., Wu, J., Wang, H., Jiang, H., & Huang, L. (2025c). Study on spatial flow field instability in a disturbing rotary centrifugal air classifier based on simulation and experimental methods. Powder Technology, 458, 120990. https://doi.org/10.1016/j.powtec.2025.120990

Liu, K., & Yu, Y. (2025). Establishment of particle motion model and study of particle volume fraction distribution in the turbo air classifier based on DSMC. Powder Technology, 120371. https://doi.org/10.1016/j.powtec.2024.120371

JIRRS
Journal International Review of Research Studies
Received: 13/06/2026 - **Accepted:** 13/11/2026
Vol: 1.11
DOI: 10.66104/gtgx0451
Pages: 1-32

Liu, K., & Yu, Y. (2024a). Study of aggregate fragmentation laws in turbo air classification flow field. CIESC Journal, 75(10), 3477–3487. https://doi.org/10.11949/0438-1157.20240470

Liu, R., Liu, J., & Yu, Y. (2015). Effects of axial inclined guide vanes on a turbo air classifier. Powder Technology, 280, 1–9. https://doi.org/10.1016/j.powtec.2015.04.034

Liu, Y., Xin, C., Tang, J., Xu, S., & Yin, Y. (2024b). CFD-DEM simulation and experimental validation of air classification for tobacco particles. Powder Technology, 448, 120318. https://doi.org/10.1016/j.powtec.2024.120318

Lu, D., Tang, Z., Fan, Y., & Lu, C. (2021). Performance of large-difference-particle air classifier. CIESC Journal, 72(8), 4184–4195. https://doi.org/10.11949/0438-1157.20201807

Lukas, E., Roloff, C., van Wachem, B., & Thévenin, D. (2020). Experimental investigation of the grade efficiency of a zigzag separator. Powder Technology, 369, 38–52. https://doi.org/10.1016/j.powtec.2020.03.001

Mann, H., Roloff, C., Hagemeier, T., Thévenin, D., & Tomas, J. (2017). Model-based experimental data evaluation of separation efficiency of multistage coarse particle classification in a zigzag apparatus. Powder Technology, 313, 145–160. https://doi.org/10.1016/j.powtec.2017.03.003

Mou, X., Jia, F., Fang, Y., & Chen, C. (2021). CFD-based structural optimization of rotor cage for high-efficiency rotor classifier. Processes, 9(7), 1148. https://doi.org/10.3390/pr9071148

Otwinowski, H., Krzywanski, J., Urbaniak, D., Wylecial, T., & Sosnowski, M. (2022). Comprehensive knowledge-driven AI system for air classification process. Materials, 15(1), 45. https://doi.org/10.3390/ma15010045

Pavlenko, I., & Yukhymenko, M. (2026). Dynamics and stability of a suspended layer in a pneumatic classifier. Applied Sciences, 16(19), 9553. https://doi.org/10.3390/app16199553

Peng, J., Hui, C., Zhao, Z., & Fang, Y. (2024). Research and optimization of operating parameters of a rotor classifier for calcined petroleum coke. Processes, 12(3), 603. https://doi.org/10.3390/pr12030603

Peng, S., Wu, Y., Tao, J., & Chen, J. (2022). Airflow velocity design for an air classifier of manufactured sand based on the CPFD method. Minerals, 12(1), 90. https://doi.org/10.3390/min12010090

Pereira, A. C. (2026a). From mineral liberation to metallurgical recovery: The role of automated mineralogy in sulfide ore processing. IKR Journal of Engineering and Technology, 2, 117–147. https://doi.org/10.5281/zenodo.20786643

JIRRS
Journal International Review of Research Studies
Received: 13/06/2026 - **Accepted:** 13/11/2026
Vol: 1.11
DOI: 10.66104/gtgx0451
Pages: 1-32

Pereira, A. C. (2026b). Scale-up in mineral processing: From mechanism preservation to flowsheet-scale transferability—A critical review and the MINESCALE framework. Journal of Advanced Multidisciplinary Studies, 1(III), 661–694. https://doi.org/10.68050/JAMS.2026.800

Petit, A., Cordoba, G., Paulo, C. I., & Irassar, E. F. (2018a). Novel air classification process for sustainable production of manufactured sands for the aggregate industry. Journal of Cleaner Production, 198, 112–120. https://doi.org/10.1016/j.jclepro.2018.07.010

Petit, H. A., & Irassar, E. F. (2021). The throat classifier: A novel air classifier for the control of dust in manufactured sands. Powder Technology, 390, 417–427. https://doi.org/10.1016/j.powtec.2021.05.049

Petit, H. A., & Irassar, E. F. (2024). Simulation of the classification of manufactured sands in the throat air classifier. KONA Powder and Particle Journal, 41, 242–253. https://doi.org/10.14356/kona.2024006

Petit, H. A., Irassar, E. F., & Barbosa, M. R. (2018b). Evaluation of the performance of the cross-flow air classifier in manufactured sand processing via CFD-DEM simulations. Computational Particle Mechanics, 5, 87–102. https://doi.org/10.1007/s40571-017-0155-6

Petit, H. A., Paulo, C. I., Cabrera, O. A., & Irassar, E. F. (2020). Modeling and optimization of an inclined plane classifier using CFD-DPM and the Taguchi method. Applied Mathematical Modeling, 77, 617–634. https://doi.org/10.1016/j.apm.2019.07.059

Ponomarev, V. B. (2025). The method of calculating the technological parameters of separation equipment for the production of fractional quartz sands. Journal of Siberian Federal University: Engineering & Technologies, 18(4), 529–537. https://www.journal.sfu-kras.ru/en/article/156186

Pukkella, A. K., Cilliers, J. J., & Hadler, K. (2023). A comprehensive review and recent advances in dry mineral classification. Minerals Engineering, 201, 108208. https://doi.org/10.1016/j.mineng.2023.108208

Qian, W., & Zeng, Y. (2026). Structural parameter effects on flow stability and classification performance in a turbo air classifier. Machines, 14(7), 765. https://doi.org/10.3390/machines14070765

Ren, J., Liu, K., Jiao, Z., Liu, J., & Yu, Y. (2023). Research on the mechanism of disaggregation of particle aggregates near the guide vanes of turbo air classifier. CIESC Journal, 74(4), 1528–1538. https://doi.org/10.11949/0438-1157.20221568

Ren, W., Liu, J., & Yu, Y. (2016a). Design of a rotor cage with non-radial arc blades for turbo air classifiers. Powder Technology, 292, 46–53. https://doi.org/10.1016/j.powtec.2016.01.024

Ren, W., Liu, J., & Yu, Y. (2016b). Design of rotor cage with arc-blade for the turbo air classifier. Journal of Mechanical Engineering, 52(2), 195–201. https://doi.org/10.3901/JME.2016.02.195

JIRRS
Journal International Review of Research Studies
Received: 13/06/2026 - **Accepted:** 13/11/2026
Vol: 1.11
DOI: 10.66104/gtgx0451
Pages: 1-32

Roloff, C., Lukas, E., van Wachem, B., & Thévenin, D. (2019). Particle dynamics investigation by means of shadow imaging inside an air separator. Chemical Engineering Science, 195, 312–324. https://doi.org/10.1016/j.ces.2018.09.020

Santos, S. J., Cho, S. G., & Lee, H. H. (2024). The study on the separation of steelmaking slags using air classification. Journal of the Korean Institute of Resources Recycling, 33(5), 51–57. https://doi.org/10.7844/kirr.2024.33.5.51

Shin, S., Kim, G., An, T., & Kim, J. (2026). Upgrading recycled concrete fines into high-value strategic resources via air classification: A dual utilization strategy for a closed-loop construction system. Sustainable Production and Consumption, 67, 184–201. https://doi.org/10.1016/j.spc.2026.06.010

Sun, Z., Liang, L., Liu, C., Yang, G. (2021a). Structural optimization of vortex finder for a centrifugal air classifier. Chemical Engineering Research and Design, 166, 220–226. https://doi.org/10.1016/j.cherd.2020.12.008

Sun, Z., Liang, L., Liu, C., Zhu, Y., Zhang, L., & Yang, G. (2021b). CFD simulation and performance optimization of a new horizontal turbo air classifier. Advanced Powder Technology, 32(4), 977–986. https://doi.org/10.1016/j.apt.2021.01.041

Sun, Z., Liu, C., Yang, G., & Chen, L. (2022). Orthogonal vortices characteristic, performance evaluation and classification mechanism of a horizontal classifier with three rotor cages. Powder Technology, 404, 117438. https://doi.org/10.1016/j.powtec.2022.117438

Sun, Z., Sun, G., & Liu, Q. (2019a). Experimental study on feeding type of horizontal turbo air classifier. China Powder Science and Technology, 25(2), 1–5. https://doi.org/10.13732/j.issn.1008-5548.2019.02.001

Sun, Z., Sun, G., Peng, P., Liu, Q., & Yu, X. (2019b). A new static cyclonic classifier: Flow characteristics, performance evaluation and industrial applications. Chemical Engineering Research and Design, 145, 141–149. https://doi.org/10.1016/j.cherd.2019.03.018

Sun, Z., Sun, G., Yang, X., Yuan, Y., Wang, Q., & Liu, J. (2017). Effects of fine particle outlet on performance and flow field of a centrifugal air classifier. Chemical Engineering Research and Design, 117, 139–148. https://doi.org/10.1016/j.cherd.2016.10.028

Tipici, V., Toprak, A., & Altun, O. (2024). Performance comparison of laboratory-scale air classifier and hydrocyclone at the same target size. Minerals Engineering, 217, 108922. https://doi.org/10.1016/j.mineng.2024.108922

Toneva, P., Epple, P., Breuer, M., Peukert, W., & Wirth, K.-E. (2011). Grinding in an air classifier mill—Part I: Characterization of the one-phase flow. Powder Technology, 211(1), 19–27. https://doi.org/10.1016/j.powtec.2011.03.009

JIRRS
Journal International Review of Research Studies
Received: 13/06/2026 - **Accepted:** 13/11/2026
Vol: 1.11
DOI: 10.66104/gtgx0451
Pages: 1-32

Vokurka, M., Zegzulka, J., Hummel, M., & Dobiáš, J. (2025). Analysis of the applicability of the Anivi-Sturtevant dynamic classifier in the production of crushed aggregates. Journal of Applied Engineering Science, 23(4), 597–606. https://doi.org/10.5937/jaes0-48844

Wang, F., Zhao, Z., Peng, J., & Fang, Y. (2025). The influence of secondary air guide vanes on the flow field and performance of a turbine air classifier. Processes, 13(7), 2268. https://doi.org/10.3390/pr13072268

Wockenfuss, L., Lammers, V., Heinz, V., Sozer, N., & Silventoinen-Veijalainen, P. (2023). Two steps of dry fractionation: Comparison and combination of air classification and electrostatic separation for protein enrichment from defatted rapeseed press cake. Journal of Food Engineering, 357, 111623. https://doi.org/10.1016/j.jfoodeng.2023.111623

Wrona, J., Żukowski, W., Bradło, D., & Czupryński, P. (2020). Recovery of cenospheres and fine fraction from coal fly ash by a novel dry separation method. Energies, 13(14), 3576. https://doi.org/10.3390/en13143576

Wu, S., Liu, J., & Yu, Y. (2017). Design of a new double layer spreading plate for a turbo air classifier. Powder Technology, 312, 277–286. https://doi.org/10.1016/j.powtec.2017.02.044

Wu, S., Liu, J., Fu, J., & Yu, Y. (2016). The design and experimental study of a double spreading disk in the turbo air classifier. Journal of Beijing University of Chemical Technology (Natural Science), 43(6), 108–113. https://doi.org/10.13543/j.bhxbzr.2016.06.017

Xie, J., Fu, J., Shao, Y., Zhang, H., Zhang, H., & Zhu, J. (2025). Narrowing the particle size distribution of powder coatings via a reformed classifying cyclone: Improved flowability and film qualities. Particuology. https://doi.org/10.1016/j.partic.2025.05.009

Xie, J., Zhu, X., Shao, Y., Zhang, H., Zhang, H., & Zhu, J. (2026). Enhancing powder coating classification accuracy via mesh-modified classifier design and operational parameter optimization. Progress in Organic Coatings, 210, 109634. https://doi.org/10.1016/j.porgcoat.2025.109634

Xing, W., Wang, Y., Zhang, Y., Yamane, Y., Saga, M., Lu, J., Zhang, H., & Jin, Y. (2015). Experimental study on velocity field between two adjacent blades and gas–solid separation of a turbo air classifier. Powder Technology, 286, 240–245. https://doi.org/10.1016/j.powtec.2015.06.044

Yan, Z., Zhang, K., Sun, Z., Wang, Z., & Yang, G. (2024). Experimental observation of the vortex flow and particle motion in a cyclonic classifier. Powder Technology, 120083. https://doi.org/10.1016/j.powtec.2024.120083

JIRRS
Journal International Review of Research Studies
Received: 13/06/2026 - **Accepted:** 13/11/2026
Vol: 1.11
DOI: 10.66104/gtgx0451
Pages: 1-32

Yang, H., Sun, Z., Liu, C., Wang, Z., Yao, Y., & Yang, G. (2023). Vortex analysis and flow field optimization for the particle classifier with three rotary cages. Advanced Powder Technology, 34(10), 104169. https://doi.org/10.1016/j.apt.2023.104169

Yoshida, T., Hirai, Y., & Sakai, S.-I. (2021). Meta-model of vertical air classification: A unified understanding of different separation curve models. Powder Technology, 383, 522–535. https://doi.org/10.1016/j.powtec.2020.10.093

Yu, L. F., Jin, Y. Q., Yuan, M. X., Zhang, F., Hu, J., Lan, J. W., Wei, Y. F., Chen, Y. M., & Ke, H. (2025). Air classification efficiency evaluation of landfilled municipal solid waste using experiments and a probabilistic method. Waste Management, 203, 114879. https://doi.org/10.1016/j.wasman.2025.114879

Yu, Y., Kong, X., & Liu, J. (2020). Effect of rotor cage's outer and inner radii on the inner flow field of the turbo air classifier. Materialwissenschaft und Werkstofftechnik, 51, 908–919. https://doi.org/10.1002/mawe.201900145

Yu, Y., Li, X., Ren, J., Kang, J., Jiao, Z., & Liu, J. (2024a). Influence of guide vane on dispersion of aggregates near the guide vane in a turbo air classifier. Powder Technology, 434, 119344. https://doi.org/10.1016/j.powtec.2023.119344

Yu, Y., Li, X., Zhang, Y., Jiao, Z., & Liu, J. (2023a). The influence of air inlet layout on the inner flow field for a vertical turbo air classifier. Physicochemical Problems of Mineral Processing, 59(6), 175859. https://doi.org/10.37190/ppmp/175859

Yu, Y., Liu, J. (2018). A parametric cut size prediction model for a turbo air classifier. Materialwissenschaft und Werkstofftechnik, 49(12), 1510–1519. https://doi.org/10.1002/mawe.201700071

Yu, Y., Liu, J., & Zhang, K. (2014). Establishment of a prediction model for the cut size of turbo air classifiers. Powder Technology, 254, 274–280. https://doi.org/10.1016/j.powtec.2014.01.009

Yu, Y., Liu, K., Li, X., Liu, J., & Jiao, Z. (2023b). Study of particle motion and distribution laws in the turbo air classification flow field. CIESC Journal, 74(10), 4074–4086. https://doi.org/10.11949/0438-1157.20230732

Yu, Y., Liu, K., Liu, X., Liu, J., Jiao, Z., & Fu, J. (2024b). Influence of feeding methods on classification performance of powder pneumatic classification and cause analyses. China Powder Science and Technology, 30(2), 36–44. https://doi.org/10.13732/j.issn.1008-5548.2024.02.004

Yu, Y., Ren, W., & Liu, J. (2019). A new volute design method for the turbo air classifier. Powder Technology, 348, 65–69. https://doi.org/10.1016/j.powtec.2019.03.015

Yuan, J., Huang, L., Li, W., Jiang, H., & Duan, C. (2024). Experimental and simulation study of flow field characteristics of a disturbing rotary centrifugal air classifier. Powder Technology, 447, 120223. https://doi.org/10.1016/j.powtec.2024.120223

JIRRS
Journal International Review of Research Studies

Received: 13/06/2026 - **Accepted:** 13/11/2026
Vol: 1.11
DOI: 10.66104/gtgx0451
Pages: 1-32

Yukhymenko, M., Ostroha, R., & Bocko, J. (2022). Design of a shelf pneumatic classifier for separating a polydisperse mixture of granulated superphosphate. Eastern-European Journal of Enterprise Technologies, 6(1), 120, 33–42. https://doi.org/10.15587/1729-4061.2022.267037

Zeng, Y., Huang, B., Qin, D., Zhou, S., & Li, M. (2022). Numerical and experimental investigation of novel guide vane structures of a turbo air classifier. Processes, 10(5), 844. https://doi.org/10.3390/pr10050844

Zeng, Y., Zhang, S., Zhou, Y., & Li, M. (2020). Numerical simulation of a flow field in a turbo air classifier and optimization of the process parameters. Processes, 8(2), 237. https://doi.org/10.3390/pr8020237

Zhao, H., Liu, J., & Yu, Y. (2018). Effects of the impeller blade geometry on the performance of a turbo pneumatic separator. Chemical Engineering Communications, 205(12), 1641–1652. https://doi.org/10.1080/00986445.2018.1464918

Zhao, Z., Hui, C., Peng, J., & Fang, Y. (2024). Influence of secondary air on the flow field of NGZF classifier. Thermal Science, 28(6A), 4637–4653. https://doi.org/10.2298/TSCI240324170Z

Zhou, Y., & Shen, W. (2022). Numerical simulation of particle classification in a new multi-product classifier. Chemical Engineering Research and Design, 177, 484–492. https://doi.org/10.1016/j.cherd.2021.11.012

Zhou, Y., Zou, X., Ma, Z., Wu, C., & Li, Y. (2024). Numerical simulation study of a pusher feed classifier based on RNG-DPM method. Processes, 12(6), 1151. https://doi.org/10.3390/pr12061151

Zhu, X., Liu, W., Zhang, H., Zhang, H., & Zhu, J. (2024). Narrowing particle size distributions to enhance powder coating performance by improved classification. Powder Technology, 119443. https://doi.org/10.1016/j.powtec.2024.119443

Zinurov, V., Kharkiv, V., Pankratov, E., & Dmitriev, A. (2022). Numerical study of vortex flow in a classifier with coaxial tubes. International Journal of Engineering and Technology Innovation, 12(4), 336–346. https://doi.org/10.46604/ijeti.2022.9568

JIRRS
Journal International Review of Research Studies

Received: 13/06/2026 - **Accepted:** 13/11/2026
Vol: 1.11
DOI: 10.66104/gtgx0451
Pages: 1-32